1-1-2020

Green synthesis and stabilization of silver nanoparticles using Lysimachia foenum-graecum Hance extract and their antibacterial activity

Widsanusan Chartarrayawadee

Phattaraporn Charoensin

Juthaporn Saenma

Thearum Rin

Phichaya Khamai

See next page for additional authors

Green synthesis and stabilization of silver nanoparticles using Lysimachia foenum-graecum Hance extract and their antibacterial activity

Abstract

2020 Chartarrayawadee et al., published by De Gruyter 2020. The Lysimachia foenumgraecum Hance extract (LHE) was used for silver nanoparticles (AgNPs) synthesis. In this study, the herbal plant of Lysimachia foenumgraecum Hance (LH) was extracted with deionized water and we are the first to successfully use LHE as reducing and stabilizing agents for the green synthesis of AgNPs. The concentration of LHE used in this study was in the range of 0.003 to 1.0 wt%. Aqueous colloidal solutions of AgNPs reduced and stabilized by LHE show long-term stability due to the steric stabilization effect. This can be confirmed by zeta potential measurements which afforded values approximately of 0 mV, indicating the steric stability of AgNPs colloidal solutions synthesized by LHE. Furthermore, the obtained AgNPs colloidal solutions show superior antibacterial effect to gram-positive bacteria (Staphylococcus aureus) comparing to Chloramphenicol (positive control). AgNPs with LHE 0.003 wt% affords the highest antibacterial effect to S. aureus showing an inhibition zone diameter of 19.08 ± 0.67 mm; which is superior to Chloramphenicol.

Disciplines

Engineering | Physical Sciences and Mathematics

Publication Details

Chartarrayawadee, W., Charoensin, P., Saenma, J., Rin, T., Khamai, P., Nasomjai, P. & Too, C. (2020). Green synthesis and stabilization of silver nanoparticles using Lysimachia foenum-graecum Hance extract and their antibacterial activity. Green Processing and Synthesis, 9 (1), 107-118.

Authors

Widsanusan Chartarrayawadee, Phattaraporn Charoensin, Juthaporn Saenma, Thearum Rin, Phichaya Khamai, Pitak Nasomjai, and Chee O. Too

Widsanusan Chartarrayawadee*, Phattaraporn Charoensin, Juthaporn Saenma, Thearum Rin, Phichaya Khamai, Pitak Nasomjai and Chee On Too

Green synthesis and stabilization of silver nanoparticles using *Lysimachia foenum-graecum* Hance extract and their antibacterial activity

https://doi.org/10.1515/gps-2020-0012
Received August 06, 2019; accepted October 30, 2019.

Abstract: The *Lysimachia foenumgraecum* Hance extract (LHE) was used for silver nanoparticles (AgNPs) synthesis. In this study, the herbal plant of *Lysimachia foenum-graecum* Hance (LH) was extracted with deionized water and we are the first to successfully use LHE as reducing and stabilizing agents for the green synthesis of AgNPs. The concentration of LHE used in this study was in the range of 0.003 to 1.0 wt%. Aqueous colloidal solutions of AgNPs reduced and stabilized by LHE show long-term stability due to the steric stabilization effect. This can be confirmed by zeta potential measurements which afforded values approximately of 0 mV, indicating the steric stability of AgNPs colloidal solutions synthesized by LHE. Furthermore, the obtained AgNPs colloidal solutions show superior antibacterial effect to gram-positive bacteria (*Staphylococcus aureus*) comparing to Chloramphenicol (positive control). AgNPs with LHE 0.003 wt% affords the highest antibacterial effect to *S. aureus* showing an inhibition zone diameter of 19.08 ± 0.67 mm; which is superior to Chloramphenicol.

Keywords: green synthesis; silver nanoparticles; *Lysimachia foenum-graecum* Hance extract; antibacterial

1 Introduction

Nanotechnology is the integration of science and technology involving the fabrication or synthesis, design and analysis of materials at the nanometer scale [1]. The control of atoms or molecules in the structure of materials at the nanometer scale allows us to adjust the properties of materials for more specific applications [2]. That is the reason why nanotechnology has received much attention from many researchers and scientists worldwide and has become more popular in both academic research and industry [3,4]. Nowadays, nanotechnology involving green synthesis of nanoparticles has become an eye-catching idea and has gained much importance and significance in recent years due to its great facility, clean processing, non-toxic chemicals used, cost-effectiveness, and being environmentally and ecofriendly. There have been many research articles focusing on the use of many kinds of plant extracts as a reducing agent for synthesis of nanoparticles; especially silver nanoparticles (AgNPs). For example, Anandalakshmi K. and co-workers used the *Pedalium murex* leaf extract for the synthesis of AgNPs and antibacterial activity has been studied. The results suggested that synthesised AgNPs had the highest antibacterial activity against *Escherichia coli* (*E. coli*) and *B. subtilis*, respectively [5]. Umadevi M. and co-workers also used the extract of *D. carota* extract for the synthesis of AgNPs [6]**.** Rajesh WR. and co-workers used the dried leaves extract of *Pongamia pinnata* (L) pierre for an extracellular synthesis of AgNPs [7]. Ghaedi M. and coworkers used the extract of *Rosmarinus officinalis* leaf and investigated its antimicrobial properties showing effective antibacterial and antifungal activities [8]. Jyoti K. and co-workers synthesized silver nanoparticles using *Urtica dioica* Linn. leaves and investigated their synergistic effects with antibiotics. The synthesized AgNPs exhibited higher activity than $AgNO_3$ solution and leaves extract [9]. Puišo J. and co-workers used lingonberry and cranberry juices in a biosynthesis of silver nanoparticles and studied their antimicrobial activity. It was found that the biosynthesized silver nanoparticles showed a broad spectrum of antimicrobial activity and were most active against *Staphylococcus aureus* (*S. aureus*), *B. subtilis* and *B. cereus* reference cultures [10]. Mražíková A. and co-workers reported the use of *P. kessleri* on the biosynthesis of AgNPs which showed a long-term stability at the higher

*** Corresponding author: Widsanusan Chartarrayawadee,** Department of Chemistry, School of Science, University of Phayao, Phayao, Thailand, email: widsanusan.ch@up.ac.th
Phattaraporn Charoensin, Juthaporn Saenma, Thearum Rin and Pitak Nasomjai, Department of Chemistry, School of Science, University of Phayao, Phayao, Thailand
Phichaya Khamai, Department of Biochemistry, School of Medical Sciences, University of Phayao, Phayao, Thailand
Chee On Too, Intelligent Polymer Research Institute, University of Wollongong, Wollongong, NSW 2522, Australia

pH values and indicated similar inhibitory antimicrobial activity as gelatin/sodium citrate-AgNPs against biofilm formation [11].

However, in this research we aimed to study the synthesis of AgNPs using a new kind of Chinese herbal plant extract called *Lysimachia foenum-graecum* Hance (LH) as a reducing and stabilizing agent to observe the stability of synthesized AgNPs. Furthermore, antibacterial property has been studied to observe the antibacterial activity of these stabilized AgNPs.

LH is a plant in *Lysimachia genus* of the *Primulaceae* family (Figure 1). It is about 50 cm tall and has a scented smell, and is mostly found in the Guangxi and Yunnan provinces of China. Commonly, it has been used to make perfume, pest repellent, alleviate pain and Chinese medical treatment for common colds and headaches [12]. However, the chemical constituent found in LH is triterpenoid saponins, flavonoids and glycosides [12,13]. Surprisingly, saponins found in LHE is the main ingredient which plays an important role in the stabilization of AgNPs in water. According to our experiment, when *Lysimachia foenum-graecum* Hance extract (LHE) was dissolved in deionized water, it produces a little foam on the solution surface. Foaming is a common and very visible effect that can occur when surfactants are present in water. Because saponins are natural surfactants showing the unique properties of foaming and emulsifying agents, they can act as a stabilizer in our experiments for AgNPs synthesis.

Figure 1: Dried *Lysimachia foenum graecum* leaf.

Surfactants or surface-active agents are large self-assembled molecular substances that possess a hydrophilic part and hydrophobic part (lipophilic part) [14,15]. Due to the amphiphilic nature of triterpenoid saponins found in LHE, they can lower surface tension (interfacial tension) and can also act as a stabilizing agent to create a high stability for metallic AgNPs in water; thus affording superior and long-term steric stabilization [16] of metallic AgNPs in colloidal solutions as can be seen in Figure 2.

Therefore, the first objective of the present study is the synthesis and characterization of AgNPs using LHE as a reducing and stabilizing agent. The investigation for the optimum concentration of LHE for the preparation of sterically stabilized colloidal solutions of AgNPs has been performed. The AgNPs were characterized by UV-Visible spectroscopy, Fourier-transform infrared spectroscopy (FTIR), Dynamic light scattering technique (DLS), X-ray diffraction (XRD) and transmission electron microscopy (TEM) measurements to observe the formation, stabilization, size and shape of AgNPs. The second objective is to evaluate the effect of green synthesized AgNPs on gram-negative and gram-positive bacteria, namely, *E. coli* and *S. aureus*, respectively using the disc diffusion method.

2 Materials and methods

2.1 Chemicals and materials

AR-grade silver nitrate ($AgNO_3$) was purchased from Labscan (RCL Labscan Limited, Bangkok, Thailand).

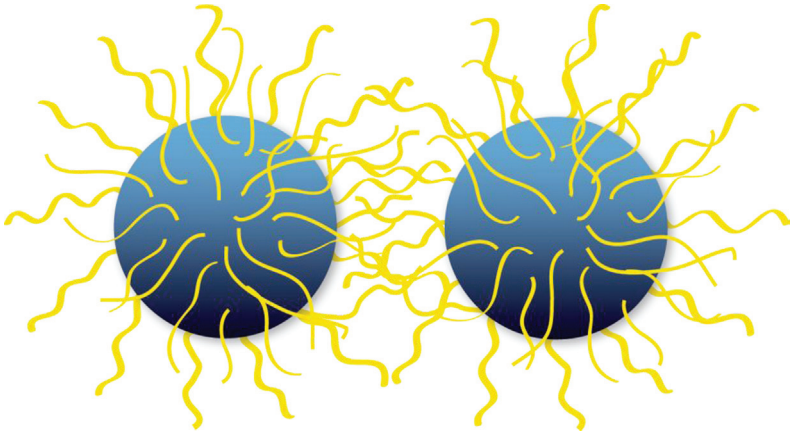

Figure 2: Steric stabilization of metallic AgNPs solution from surfactants found in LHE.

Dried leaves of *Lysimachia foenum-graecum* Hance were imported from China. The nutrient agar (Muller Hinton agar (MHA) and Muller Hinton broth (MHB) were purchased from HiMedia Laboratories (HiMedia Laboratories Pvt. Ltd. Mumbai, India). Deionized water (RCL Labscan Limited, Bangkok, Thailand) was used in all the experiments.

2.2 Preparation of *Lysimachia foenum-graecum* - Hance extract

100 g of LH dried leaves were cut into small pieces in a Moulinex blender and were boiled for 3 h at 80°C with deionized water. The ratio of LH dried leaves to deionized water was 1 g : 10 mL after boiling for 3 h. The solution was then filtered and lyophilized to obtain brown extracted powder. The LHE was used as a reducing agent and stabilizing agent.

2.3 Silver nanoparticles synthesis

The green synthesis of AgNPs with LHE as a reducing and stabilizing agent was performed as follows: Solution of silver nitrate 25 mL, 0.025 wt% of Ag was added into 25 mL of LHE solution. The concentration of LHE in the mixture was prepared as follows: 0.003 wt%, 0.01 wt%, 0.05 wt%, 0.1 wt%, 0.5 wt% and 1.0 wt%. The solution mixture was then stirred until it became homogeneous. The reaction mixture was stirred overnight (12 h) at room temperature and the temperature was increased to 90°C for 1 h in the final reaction process. The AgNPs formation was observed by the appropriate color change and had been kept in the dark condition at room temperature prior to use.

2.4 Antimicrobial activity

The synthesized AgNPs were tested for antimicrobial activity using the disc diffusion method following standards and guidelines from the Clinical Laboratory Standards Institute (CLSI). The overnight-grown bacteria used in this study were gram-positive *S. aureus* (ATCC 25923) and gram-negative *E. coli* (ATCC 25922) which were standardized using McFarland standard (McFarland standard No. 0.5). These microorganisms were collected, cultured and maintained at the Department of medical microbiology and parasitology, School of Science, University of Phayao, Phayao, Thailand. The bacteria suspensions were diluted 1:10 to obtain 1.5×10^7 colony forming units per milliliter (CFU/mL) and were plated on the nutrient agar using sterile cotton buds. Whatman filter paper (no:1) discs of 75 mm diameter were dipped in $AgNO_3$ 0.025 wt%, LHE 1.0 wt% and different dilutions of biosynthesized AgNPs varying from 0.003 wt%, 0.01 wt%, 0.05 wt%, 0.1 wt%, 0.5 wt% and 1.0 wt%. Each Petri plate containing nutrient agar was loaded with four antibacterial testing samples. The Petri plates were incubated at 37°C for 12 h and then examined for the appearance of a clear area around the disc by measuring the diameter of inhibition zones using a ruler which was recorded and expressed in millimeters.

2.5 Sample characterization

UV-Visible (UV-Vis) absorption measurements were performed using a UV-Vis spectrometer (Jusco, V530, Jasco International Co., Ltd., Tokyo, Japan) in dual beam mode. Fourier-transform infrared (FTIR) data were collected using an FTIR spectrometer (Nicolet 6700, Thermo Fisher Scientific). A laser particle sizer (Malvern Zetasizer Nano ZS, Malvern Instruments limited, Worcestershire, UK) equipped with a He-Ne laser at 633 nm, 4 mW was used to determine particle size and zeta potential at 25°C by dynamic light scattering (DLS) in back scattering mode. An X-ray diffractometer (Rigaku Miniflex 600 X-ray diffractometer using Cu Kα x-ray radiation, Rigaku Corporation, Tokyo, Japan) was used to obtain the diffraction patterns of the AgNPs on a glass slide. A transmission electron microscope (TEM, Philips Tecnai 12, FEI Company, OR, USA) was used to investigate the size and morphology of AgNPs.

3 Results and discussion

3.1 Spectroscopic measurements

UV-Vis spectroscopy was employed to investigate the formation and stabilization of AgNPs in aqueous solution containing LHE. The AgNPs solutions were subjected to test on the first day after heat treatment. It can be observed that, the absorbance intensity of AgNPs gradually reduced with respect to the concentration of LHE used in the reduction process from 0.003 wt%, 0.01 wt%, 0.05 wt%, 0.1 wt%, 0.5 wt% and 1.0 wt% (Figure 3). The absorbance peaks appeared around λ_{max} = 410-430 nm for the whole concentration range of 0.003-1.0 wt% of LHE resulting from the excitation of the surface plasmon vibration in the AgNPs; indicating the formation of AgNPs in this

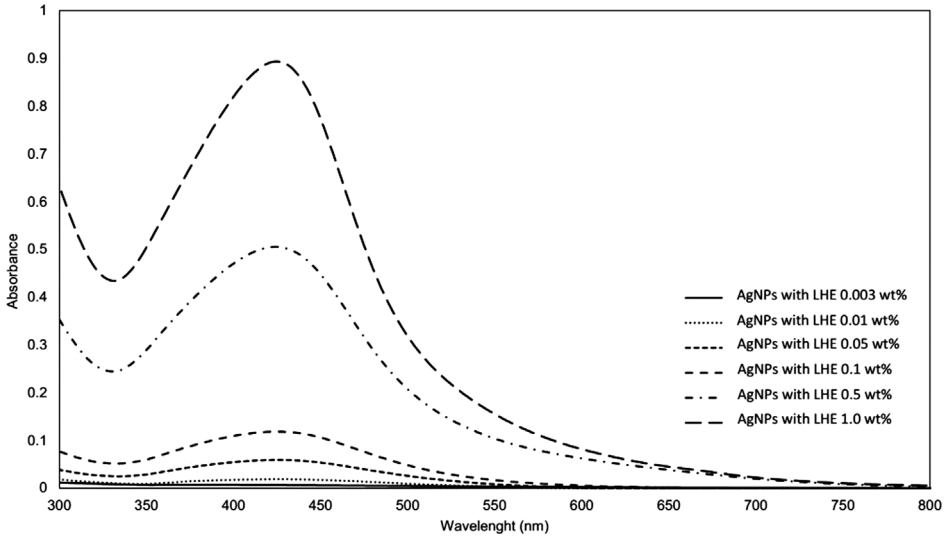

Figure 3: UV-Vis spectra of AgNPs reduced by LHE concentration vary from 0.003 wt% to 1.0 wt%.

experiment. Shifting of surface plasmon bands at around 410 to 430 nm [17,18] depends on some factors such as size and shape of AgNPs. The peak position and peak shape of AgNPs in Figure 3 can be used roughly to predict the size and shape of AgNPs indicating that they are quasi-spherical in shape and AgNPs size should be approximately around 10 to 20 nm [19-21]. It can also be seen that when the LHE concentration increased, the absorbance intensity also increased. This can be interpreted that the functional groups in LHE help to promote the reduction of silver metal ions in aqueous solution.

Figure 4 shows color intensity of $AgNO_3$ aqueous solution with LHE before the reduction process takes place (Figure 4a), AgNPs colloidal solution after overnight reduction (Figure 4b) and AgNPs colloidal solution after overnight reduction followed by heating at 90°C for 1 h (Figure 4c). To make a clearer observation, the dilution series of colloidal solution in each figure (Figures 4a-c) which were labeled as A1 to A10, B1 to B10 and C1 to C10 represent the concentration of LHE in the concentration range from 0.003 wt%, 0.006 wt%, 0.01 wt%, 0.025 wt%, 0.05 wt%, 0.08 wt%, 0.1 wt%, 0.3 wt%, 0.5 wt% and 1.0 wt%. It can be seen that the solution color in Figures 4b and 4c changed from light yellow to pale orange, orange, dark orange, brown, and dark brown and the colors are more intense than the solution in Figure 4a; indicating the formation of AgNPs colloidal solution and plasmon resonance absorption. This result corresponds to the UV-Vis spectra in Figure 3 that the color intensity and absorbance intensity of AgNPs colloidal solutions increased with the reduction process taking place. Furthermore, the reduction process of AgNPs by LHE can proceed faster and completely achieved by heating.

Figure 5 shows the UV-Vis spectra of colloidal solution of AgNPs reduced by LHE to observe the stability of the series of colloidal solutions ranging from 0.003 to 1.0 wt%. The observations were made on the 2nd, 3rd, 4th and 10th week and the AgNPs solution has been kept in the dark condition at room temperature. It can be noticed that good UV-Vis spectra were observed until the 10th week which confirms the stability of AgNPs colloidal solution reduced by LHE. Furthermore, after the AgNPs colloidal solutions had been kept for more than 6 months, they still showed good stability of AgNPs colloidal dispersion, thus indicating the superior dispersion of this AgNPs colloidal system. These results are superior to the work published by Velgosova O. and co-workers [22], where the biologically synthesized AgNPs using algae *Parachlorella kessleri* stored in the dark at room temperature showed better long-term stability but weak particle agglomeration was observed at approximately the 100th day. Furthermore, the stability of our biologically synthesized AgNPs using LHE can be stored without chemical stabilizer such as polyvinyl alcohol (PVA) [23].

Figure 6 shows FTIR spectra of pure LHE and dried powder obtained from AgNPs colloidal solutions at the different LHE concentrations. FTIR spectra of LHE show a broad peak at around 3300 cm^{-1}, which is attributed to the –OH functional group (H-bond stretching). Some other peaks at 2927 cm^{-1} and 1386 cm^{-1} can also be observed, which can be attributed C-H stretching vibration and C–H bending vibration respectively. The remaining two others at 1590 cm^{-1} and 1022 cm^{-1} also observed can be attributed to C=C stretching vibrations in the aromatic ring and oligosaccharide linkage absorptions to sapogenins C–O–C, respectively. As we mentioned earlier, saponins

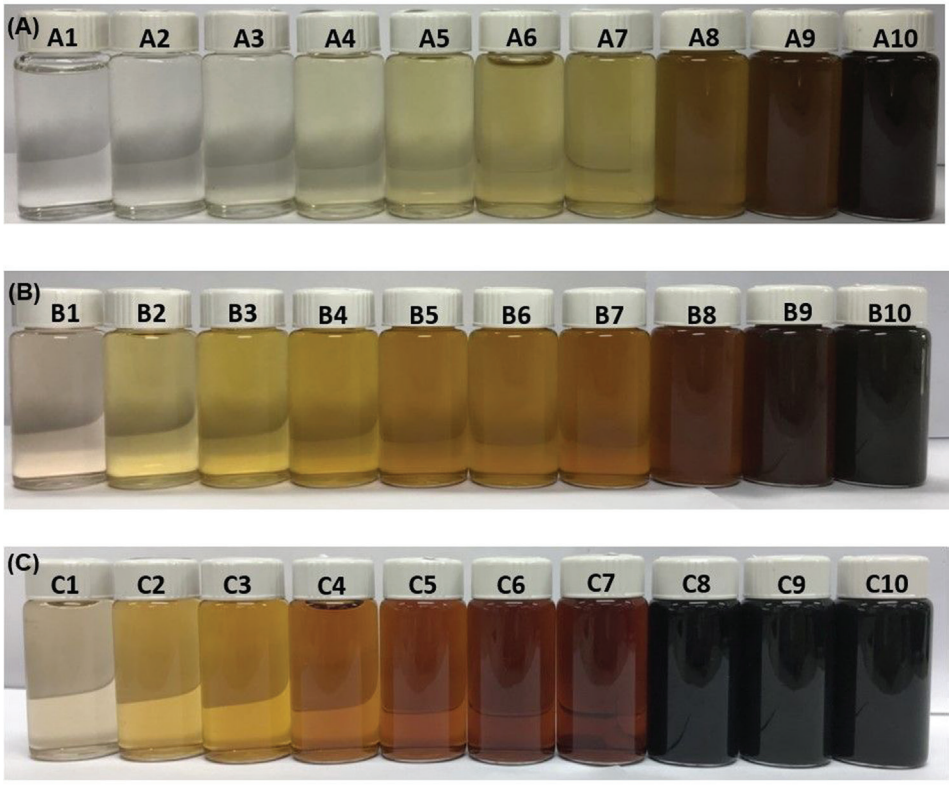

Figure 4: Changing of color intensity of AgNPs aqueous solution reduced by LHE before reduction process takes place (a), after overnight reduction (b), and after overnight reduction followed by heating at 90°C for 1 h (c). Numbers 1 to 10 represent the employed concentration range of LHE: 0.003 wt%, 0.006 wt%, 0.01 wt%, 0.025 wt%, 0.05 wt%, 0.08 wt%, 0.1 wt%, 0.3 wt%, 0.5 wt% and 1.0 wt%.

found in LHE is the main ingredient which plays an important role in the stabilization of AgNPs in water. These results agree with the FTIR spectra of saponins in crude extract of soapnuts reported by Meshari et al. [24]. It can also be observed that the high similarity between LHE and AgNPs reduced by LHE indicated the same compounds existed in all samples. The FTIR spectra of saponin in LHE and AgNPs reduced by LHE demonstrated the characteristic of triterpenoid saponin absorptions of –OH, C–H, and C=C, while the absorptions of C–O–C indicated the glycoside linkages to the sapogenins. It should be noted that the extract consists of differences in saponin content and composition. In general, saponins consist of a hydrophobic aglycone structure with hydrophilic sugar residues linkage. The steric stabilization mechanism of the AgNPs depends on the extensive hydration of the hydrophilic sugar residues in the adsorbed saponin layer [25,26]. Furthermore, it can be observed that as the concentration of LHE was increased, clear peaks in the spectra were revealed. The marked shifts at 3300 cm^{-1}, 1386 cm^{-1} and 1022 cm^{-1} also observed are related to the adsorption of LHE constituents on the AgNPs surface which are aiding the reduction and stabilization of AgNPs.

3.2 X-ray diffraction

The powder of AgNPs obtained from AgNPs colloidal solution by the reduction of LHE (after heat treatment) at the different concentrations of 0.003, 0.01, 0.05, 0.1, 0.5 and 1.0 wt% were subjected to analysis of their crystalline nature through X-ray diffraction. A comparison of our XRD spectrum with the standard confirmed that AgNPs in our experiment were in the form of nanocrystals, as evidenced by the XRD patterns showing four diffraction peaks at 2θ values of around 38°, 44°, 64° and 78° which are indexed as the (111), (200), (220) and (311) Bragg reflections, respectively. These diffraction peaks are well consistent with the standard data file (JCPDS No. 04-0783) and can be indexed as the face-centered cubic structure of silver (Figures 7a-f). XRD patterns of the synthesized AgNPs show a strong diffraction peak corresponding to the (200) facet at the first few synthesis conditions (0.003 and 0.01 wt% of LHE) while the others show a strong diffraction peak corresponding to the (111) facet; especially at the high LHE concentration range (0.1 to 1.0 wt%). These results suggest the predominance of (111) plane orientation of AgNPs in the synthesis condition of 0.01 to 1.0 wt% of LHE.

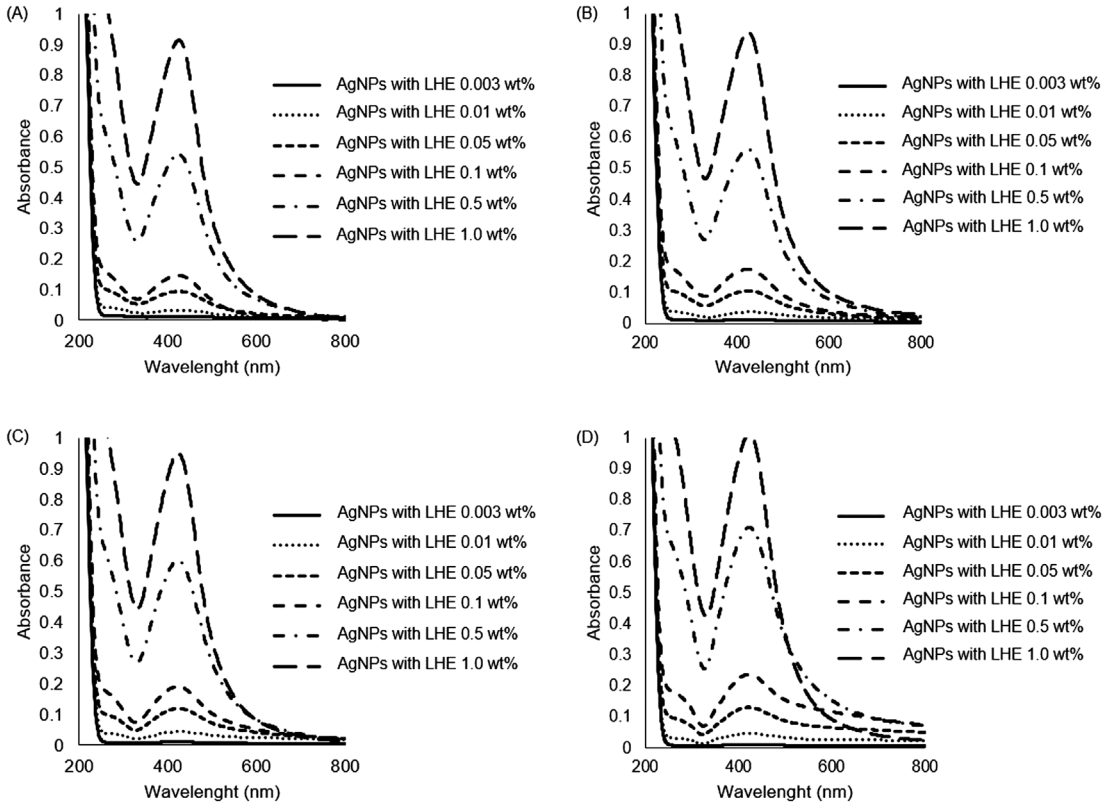

Figure 5: (a) to (d) represent UV-Vis spectra of different AgNPs colloidal solutions reduced and stabilized with LHE measured at: (a) week 2, (b) week 3, (c) week 4 and (d) week 10.

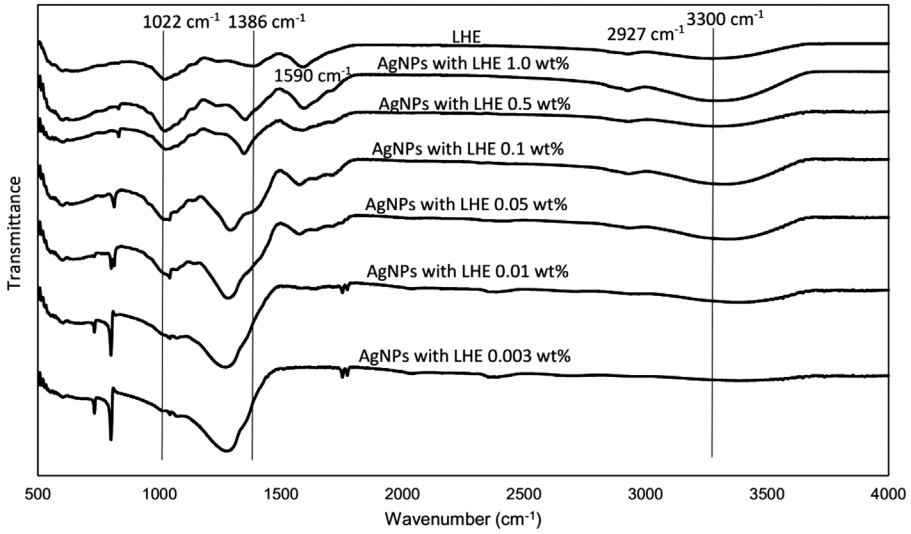

Figure 6: FTIR of LHE and silver nanoparticles obtained using the LHE extract.

3.3 Zeta potential and size distribution

To observe the charge on the particle surface and particle size of AgNPs, Dynamic Light Scattering (DLS) technique was used to determine the zeta potential and size of AgNPs. Surprisingly, AgNPs colloidal solutions obtained from LHE reduction at the concentration of 0.003 to 1.0 wt% show zeta potential values of approximately zero in all samples as shown in Table 1. This result indicates that the stability of AgNPs colloidal solution obtained from LHE reduction is not due to electrostatic stabilization but is due to steric stabilization afforded

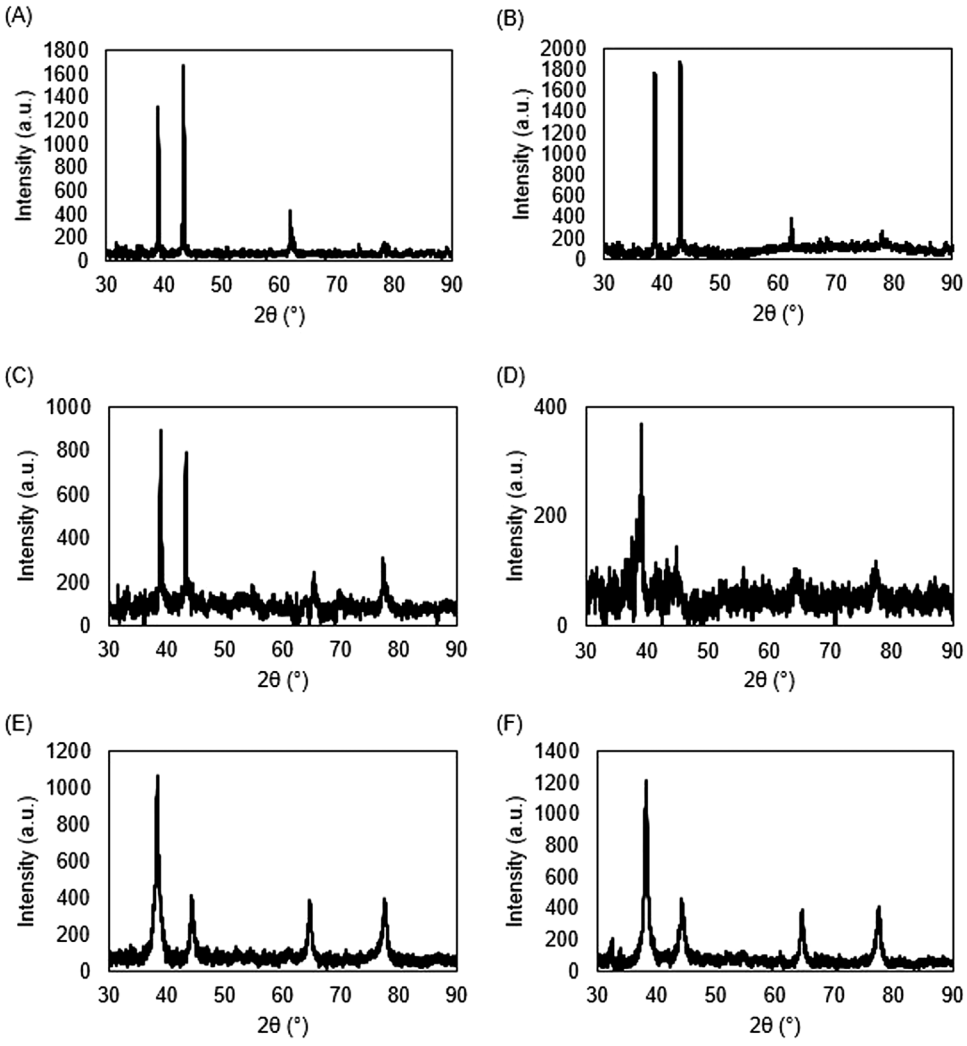

Figure 7: Powder XRD pattern of silver nanoparticles (AgNPs) obtained from AgNPs colloidal solution using LHE at the different concentrations: (a) 0.003 wt%, (b) 0.01 wt%, (c) 0.05 wt%, (d) 0.1 wt%, (e) 0.5 wt%, and (f) 1.0 wt%, respectively.

Table 1: Zeta potentials and particles sizes of AgNPs colloidal solutions obtained from LHE reduction (after heat treatment) at the concentration range between 0.003 to 1.0 wt%.

LHE concentration (wt%)	Mean zeta potential (mV)	Mean particle size (1st peak-nm)	Mean particle size (2nd peak-nm)	Mean particle size (3rd peak-nm)
0.003	0.0060 ± 0.0570	-	175 ± 71	-
0.01	−0.0085 ± 0.0184	12 ± 3	108 ± 61	4241 ± 990
0.05	0.0019 ± 0.0697	15 ± 3	95 ± 50	4676 ± 793
0.1	−0.0179 ± 0.1369	11 ± 3	106 ± 65	3285 ± 1233
0.5	0.0355 ± 0.0656	21 ± 5	140 ± 72	4710 ± 769
1.0	−0.0386 ± 0.0723	11 ± 3	158 ±76	4800 ± 726

by the natural surfactants in LHE as we had described earlier and also shown in Figure 2. In terms of particle size, it can be observed that the AgNPs colloidal solution with LHE concentration of 0.003 wt% shows a peak of mean particle size (175 ± 71 nm); while other AgNPs with LHE concentrations of 0.01, 0.05, 0.1, 0.5 and 1.0 show three different mean particle sizes as shown in Table 1. It can be observed that, the first and second peak represent the small and large size of AgNPs obtained from the reduction while the third peak might be the size

of the self-assembled surfactant aggregates or *surfactant micelle that existed at high concentrations of LH*E (0.01 to 1.0 wt%). However, particle sizes obtained using Dynamic Light Scattering (DLS) and TEM are different. DLS gives the hydrodynamic size (the size of the nanoparticle plus the liquid layer around the particle) while TEM gives the actual size of the nanoparticle [27,28]. This is the reason to explain why size measured by DLS is different from TEM. Thus, the mean particle size at the 2nd peak of LHE 0.03, 0.01, 0.05, 0.1, 0.5 and 1.0 wt% (175 ± 71 nm, 108 ± 61 nm, 95 ± 50 nm, 106 ± 65 nm, 140 ± 72 nm and 158 ± 76 nm, respectively) should be the hydrodynamic diameters of AgNPs coated with phytochemicals (hydrodynamic radius) because phytochemicals coatings on AgNPs are resulting in substantial changes in the hydrodynamic radius. This result suggests that the phytochemicals (triterpenoid saponins, flavonoids and glycosides) found in LHE are capped on AgNPs. Furthermore, only one mean particle size at the 2nd peak of LHE 0.003 wt% was observed at this condition representing the optimized concentration for AgNPs synthesis resulting in good antibacterial activity to *S. aureus* which will be discussed in the last section. However, the mean particle size at the 1st peak of LHE 0.003 wt% was not observed, which may be due to the concentration of AgNPs in solution being too low.

3.4 TEM morphology

TEM images of AgNPs prepared by the green reduction using LHE of concentration range from 0.003 to 1.0 wt% are shown in Figure 8. It can be observed that at the lowest LHE concentration of 0.003 wt%, the AgNPs size observed by TEM is approximately 20 nm in size (Figure 8a). When the LHE concentration is increased (0.01 to 1.0 wt%), the combination of AgNPs size range started to appear as shown in Figures 8b-f. This result corresponds to the result observed by DLS that multiple peaks of mean particle size were observed at LHE concentration range from 0.01 to 1.0 wt%. Furthermore, it should be noted that there is no big difference in the particle size of AgNPs which were observed by TEM in all synthesis conditions which is in keeping with the DLS technique which also showed no big difference in particle size observed. However, as we mentioned in the previous section, the particle size of AgNPs determined by DLS and TEM are different due to the enveloped state of particles in media. DLS gives a hydrodynamic diameter/radius, while TEM gives an actual particle size in the dry state. Thus, the size obtained by these two characterization techniques are different. Furthermore, it should be noted that surfactants can influence or possess ability to control crystal growth [29,30]. This is the reason to explain why the size of nanoparticles do not vary outstandingly with the concentration of plant extract in this experiment. This is because nanoparticles are capped by surfactants found in phytochemicals in LHE.

3.5 Antimicrobial activity

The antibacterial activity of synthesized AgNPs were subjected to test with gram-negative bacteria *E. coli* and gram-positive *S. aureus*. AgNPs in all synthesis conditions were tested for antibacterial activity comparing with pure DI water (negative control), Chloramphenicol (positive control), pure LHE and $AgNO_3$ (equivalent to 0.025 wt% of Ag). Figure 9 shows the position measurement of inhibition zone. The negative control and positive control were measured in each condition for comparison. The inhibition zone (average value ± standard deviation) of pure LHE, $AgNO_3$ and AgNPs at the different concentrations of LHE were measured 6 times in each experiment (labelled with numbers 1 to 6). The inhibition zone diameters of all samples are recorded in Table 2. It should be noted that the negative control (DI water) and pure LHE show no antibacterial activity while the positive control (Chloramphenicol) and $AgNO_3$ (0.025 wt% of Ag) show the inhibition zone diameter of 18.88 ± 1.00 mm and 15.33 ± 0.89 mm for *E. coli* and 14.93 ± 0.40 mm and 15.08 ± 0.1 mm for *S. aureus*, respectively. In terms of antibacterial activity to *E. coli*, most AgNPs at different LHE concentrations show less antibacterial activity when compared to Chloramphenicol and $AgNO_3$. In contrast, a stronger antibacterial effect to *S. aureus* comparing to Chloramphenicol and $AgNO_3$ was observed in most cases of synthesized AgNPs. Notably, AgNPs with LHE 0.003 wt% demonstrated a superior antibacterial effect; affording the highest inhibition zone diameter of 19.08 ± 0.67 mm. This value is much higher than Chloramphenicol and $AgNO_3$. This result can be explained by the average AgNPs size with LHE 0.003 wt% observed by TEM which shows less distribution in size of approximately to 20 nm while the others show a variation in size with large particles or agglomerations. The smaller size of AgNPs affords a higher surface area (large surface/volume ratio), which is considered to be more effective than larger particles, resulting in a superior effective binding to the bacterial membrane or ease to reach cellular proximity [31-33]. The superior antibacterial activity of AgNPs at this condition

(LHE 0.003 wt%) suggests this condition to be optimal for the green synthesis of AgNPs in this system. However, a major difference in the inhibition zone between $AgNO_3$ and green-synthesized AgNPs with LHE 0.003 wt% to *S. aureus* might be explained by previous findings that silver ions produced in an electrolytic way are better antibacterial agents than dissolved silver compounds [34,35]. While in the case of *E. coli*, a small difference in the inhibition zone can be observed due to the negatively charged lipopolysaccharide which makes Gram-negative bacteria more resistant than the Gram-positive bacteria [36,37].

4 Conclusions

In this research, we are the first to successfully synthesize AgNPs by green synthesis using *Lysimachia foenum-graecum* Hance extract (LHE) as reducing and stabilizing agent. Synthesized AgNPs with different LHE

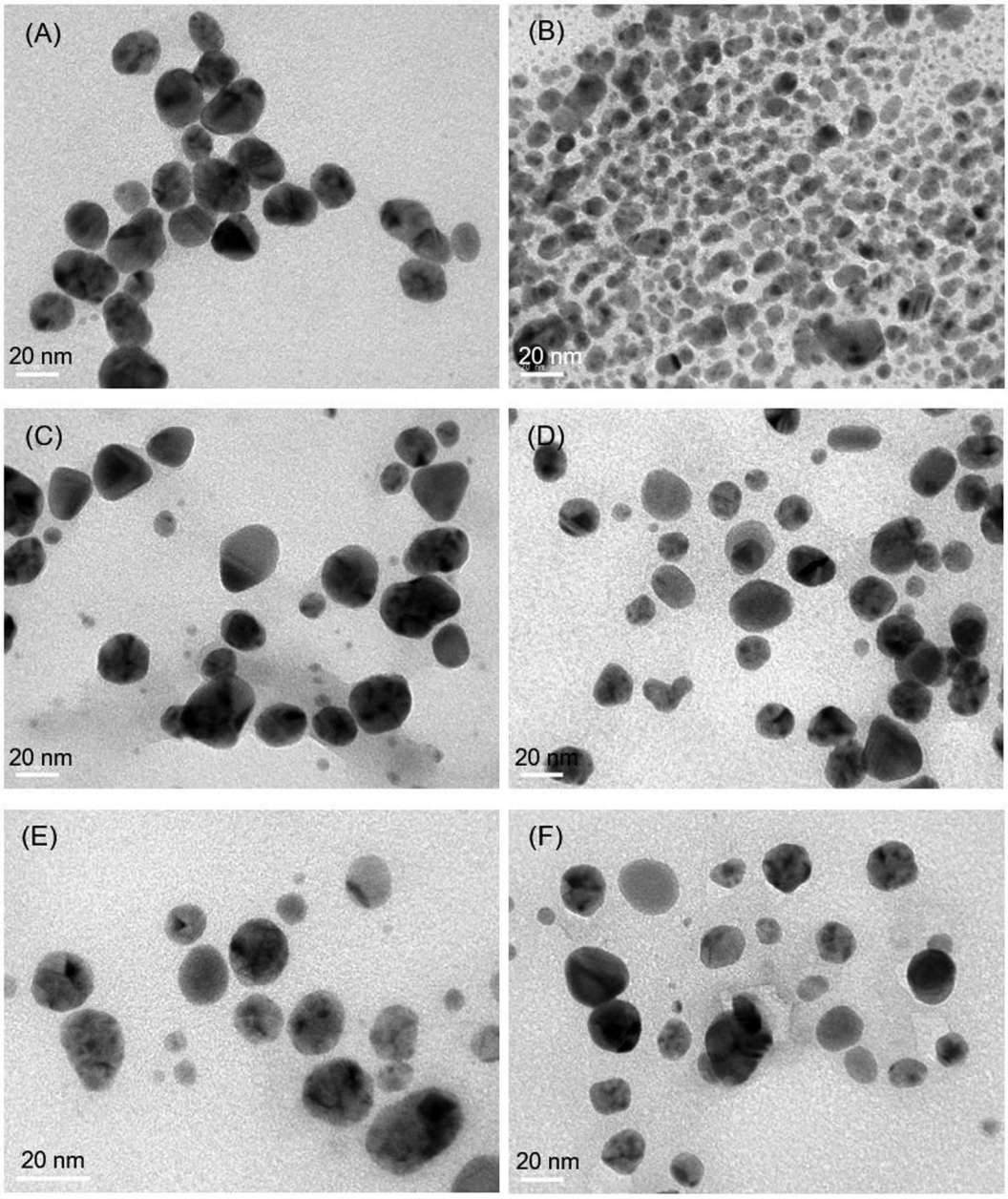

Figure 8: Show TEM images of silver nanoparticles prepared with different LHE concentrations: (a) 0.003 wt%, (b) 0.01 wt%, (c) 0.05 wt%, (d) 0.1 wt%, (e) 0.5 wt% and (f) 1.0 wt%, respectively.

concentrations show quasi-spherical shape with long term stability in water. In this experiment, it can be seen that LHE can be used as a reducing and superior long-term stabilizing agent for AgNPs. Furthermore, AgNPs aqueous colloidal solutions show advantage in antimicrobial activity. AgNPs with LHE 0.003 wt% (smallest LHE concentration) affords the highest antibacterial effect to *S. aureus* showing an inhibition zone diameter of 19.08 ± 0.67 mm; which is superior to Chloramphenicol. The results suggest that synthesizing AgNPs by using LHE is a facile pathway, cost-effective, safe to the environment and living organisms and also shows a superior stability with outstanding antimicrobial activity to *S. aureus*.

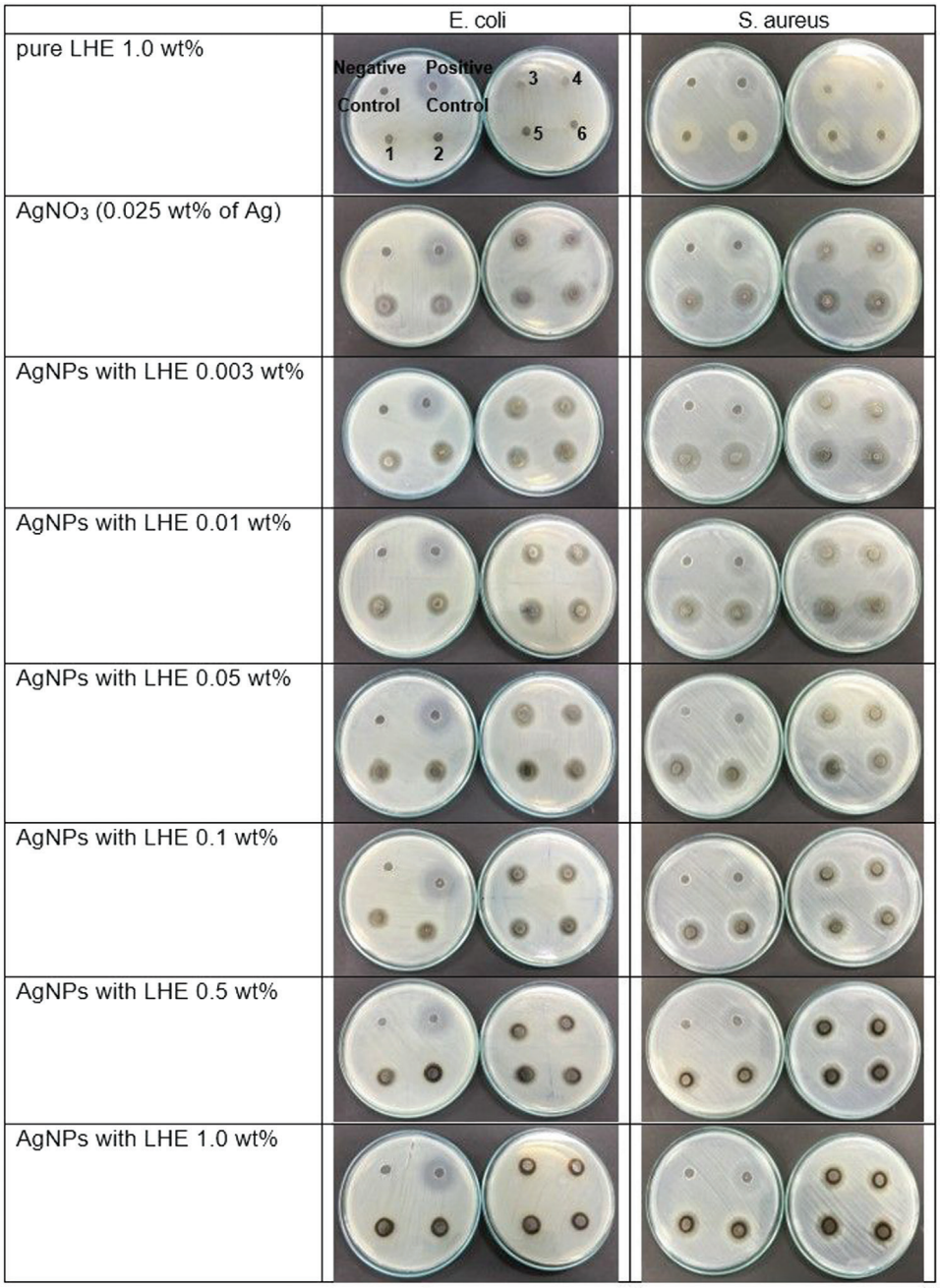

Figure 9: The inhibition zone of negative and positive control (labelled by negative control and positive control) comparing with the inhibition zone of pure LHE, $AgNO_3$ and AgNPs at the different LHE concentrations (labelled with numbers 1 to 6). The labels are applied to all figures in every condition for both *E. coli* and *S. aureus*.

Table 2: The record of inhibition zone diameter (average value ± standard deviation) of all samples listed in Figure 9.

Sample	Inhibition zone diameter (mm)	
	E. coli	*S. aureus*
DI water (negative control)	0.00 ± 0.00	0.00 ± 0.00
Chloramphenicol (positive control)	18.88 ± 1.00	14.93 ± 0.40
LHE 1.0 %wt	0.00 ± 0.00	0.00 ± 0.00
$AgNO_3$ (0.025 wt% of Ag)	15.33 ± 0.89	15.08 ± 0.1
AgNPs with LHE 0.003 wt%	15.58 ± 0.51	19.08 ± 0.67
AgNPs with LHE 0.01 wt%	14.75 ± 0.97	18.17 ± 0.94
AgNPs with LHE 0.05 wt%	14.08 ± 0.1	16.27 ± 0.79
AgNPs with LHE 0.1 wt%	13.00 ± 0.00	14.67 ± 0.98
AgNPs with LHE 0.5 wt%	12.83 ± 1.19	16.92 ± 1.24
AgNPs with LHE 1.0 wt%	12.36 ± 0.50	17.33 ± 0.49

Acknowledgement: The authors would like to thank the Biodiversity-Based Economy Development Office (Public Organization), National Research Council of Thailand, Thailand's Office of the Higher Education Commission, and the University of Phayao, Thailand for their financial support.

References

[1] Liddle J.A., Gallatin G.M., Nanomanufacturing: A Perspective. ACS Nano, 2016, 10(3), 2995-3014.

[2] Henzie J., Barton J.E., Stender C.L., Odom T.W., Large-Area Nanoscale Patterning: Chemistry Meets Fabrication. Accounts Chem. Res., 2006, 39(4), 249-257.

[3] Liddle J.A., Gallatin G.M., Lithography, metrology and nanomanufacturing. Nanoscale, 2011, 3(7), 2679-2688.

[4] Velev O.D., Gupta S., Materials Fabricated by Micro- and Nanoparticle Assembly – The Challenging Path from Science to Engineering. Adv. Mater., 2009, 21(19), 1897-1905.

[5] Anandalakshmi K., Venugobal J., Ramasamy V., Characterization of silver nanoparticles by green synthesis method using *Pedalium murex* leaf extract and their antibacterial activity. Appl. Nanosci., 2016, 6(3), 399-408.

[6] Umadevi M., Shalini S., Bindhu M.R., Synthesis of silver nanoparticle using *D. carota* extract. Adv. Nat. Sci.-Nanosci., 2012, 3(2), 025008.

[7] Rajesh W.R., Niranjan S.K., Jaya R.L., Vijay D.M., Sahebrao B.K., Extracellular synthesis of silver nanoparticles using dried leaves of *Pongamia pinnata* (L) pierre. Nano-Micro Lett., 2010, 2(2), 106-113.

[8] Ghaedi M., Yousefinejad M., Safarpoor M., Khafri H.Z., Purkait M.K., *Rosmarinus officinalis* leaf extract mediated green synthesis of silver nanoparticles and investigation of its antimicrobial properties. J. Ind. Eng. Chem., 2015, 31, 167-172.

[9] Jyoti K., Baunthiyal M., Singh A., Characterization of silver nanoparticles synthesized using *Urtica dioica* Linn. leaves and their synergistic effects with antibiotics. J. Radiat. Res. Appl. Sci., 2016, 9(3), 217-227.

[10] Puišo J., Jonkuvienė D., Mačionienė I., Šalomskienė J., Jasutienė I., Kondrotas R., Biosynthesis of silver nanoparticles using lingonberry and cranberry juices and their antimicrobial activity. Colloid. Surface. B, 2014, 121, 214-221.

[11] Mražíková A., Velgosová O., Kavuličová J., Krum S., Malek J., The influence of silver nanoparticles synthesis on their properties. Acta Polytech., 2018, 58, 365-369.

[12] Shen Y.H., Weng Z.Y., Zhao Q.S., Zeng Y.Q., Ríos J.L., Xiao W.L., et al., Five New Triterpene Glycosides from *Lysimachia foenum-graecum* and Evaluation of their Effect on the Arachidonic Acid Metabolizing Enzyme. Planta Med., 2005, 71(08), 770-775.

[13] Veitch N.C., Grayer R.J., Flavonoids and their glycosides, including anthocyanins. Nat. Prod. Rep., 2008, 25(3), 555-611.

[14] Walthelm U., Dittrich K., Gelbrich G., Schöpke T., Effects of Saponins on the Water Solubility of Different Model Compounds. Planta Med., 2001, 67(01), 49-54.

[15] Güçlü-Üstündağ Ö., Mazza G., Saponins: Properties, Applications and Processing. Crit. Rev. Food Sci., 2007, 47(3), 231-258.

[16] Parfitt G.D., Barnes H.A., Chapter 6 - The dispersion of fine particles in liquid media. In: Harnby N., Edwards M.F., Nienow A.W. (Eds.), Mixing in the Process Industries (2nd ed.). Butterworth-Heinemann, Oxford, 1992.

[17] Amaladhas D.T., Usha M., Shivanna N., Sunlight induced rapid synthesis and kinetics of silver nanoparticles using leaf extract of *Achyranthes aspera* L. and their antimicrobial applications. Adv. Mater. Lett., 2013, 4(10), 779-785.

[18] El-Zahry M.R., Mahmoud A., Refaat I.H., Mohamed H.A., Bohlmann H., Lendl B., Antibacterial effect of various shapes of silver nanoparticles monitored by SERS. Talanta., 2015, 138, 183-189.

[19] Tanvi, Mahajan A., Bedi R.K., Kumar S., Saxena V., Singh A., et al., Broadband enhancement in absorption cross-section of N719 dye using different anisotropic shaped single crystalline silver nanoparticles. RSC Adv., 2016, 6(53), 48064-48071.

[20] Raza M.A., Kanwal Z., Rauf A., Sabri A.N., Riaz S., Naseem S., Size- and Shape-Dependent Antibacterial Studies of Silver Nanoparticles Synthesized by Wet Chemical Routes. Nanomaterials-Basel., 2016, 6(4), 74.

[21] Mukherji S., Bharti S., Shukla G., Mukherji S., Synthesis and characterization of size- and shape-controlled silver nanoparticles. Phys. Sci. Rev. (in press), DOI:10.1515/psr-2017-0082.

[22] Velgosova O., Čižmárová E., Málek J., Kavuličova J., Effect of storage conditions on long-term stability of Ag nanoparticles formed via green synthesis. Int. J. Min. Met. Mater., 2017, 24(10), 1177-1182.

[23] Ardani H.K., Imawan C., Handayani W., Djuhana D., Harmoko A., Fauzia V., Enhancement of the stability of silver nanoparticles synthesized using aqueous extract of *Diospyros discolor* Willd. leaves using polyvinyl alcohol. IOP Conf. Ser. Mater. Sci. Eng., 2017, 188, 012056.

[24] Almutairi M.S., Ali M., Direct detection of saponins in crude extracts of soapnuts by FTIR. Nat. Prod. Res., 2015, 29(13), 1271-1275.

[25] Wojciechowski K., Orczyk M., Marcinkowski K., Kobiela T., Trapp M., Gutberlet T., et al. Effect of hydration of sugar groups on adsorption of Quillaja bark saponin at air/water and Si/water interfaces. Colloid. Surface. B, 2014, 117, 60-67.

[26] Sarnthein-Graf C., La Mesa C., Association of saponins in water and water–gelatine mixtures. Thermochim. Acta, 2004, 418(1), 79-84.

[27] Nune S.K., Chanda N., Shukla R., Katti K., Kulkarni R.R., Thilakavathy S., et al., Green nanotechnology from tea: phytochemicals in tea as building blocks for production of biocompatible gold nanoparticles. J. Mater. Chem., 2009, 19(19), 2912-2920.

[28] Domingos R.F., Baalousha M.A., Ju-Nam Y., Reid M.M., Tufenkji N., Lead J.R., et al., Characterizing Manufactured Nanoparticles in the Environment: Multimethod Determination of Particle Sizes. Environ. Sci. Technol., 2009, 43(19), 7277-7284.

[29] Bakshi M.S., How Surfactants Control Crystal Growth of Nanomaterials. Cryst. Growth Des., 2016, 16(2), 1104-1133.

[30] Heinz H., Pramanik C., Heinz O., Ding Y., Mishra R.K., Marchon D., et al., Nanoparticle decoration with surfactants: Molecular interactions, assembly, and applications. Surf. Sci. Rep., 2017, 72(1), 1-58.

[31] Yuan Y.G., Peng Q.L., Gurunathan S., Effects of Silver Nanoparticles on Multiple Drug-Resistant Strains of *Staphylococcus aureus* and *Pseudomonas aeruginosa* from Mastitis-Infected Goats: An Alternative Approach for Antimicrobial Therapy. Int. J. Mol. Sci., 2017, 18(3), 569.

[32] Alizadeh V., Golestani Eimani B., Amjady F., Genomic Effect of Silver Nanoparticles in *Staphylococcus aureus* Bacteria. J. Water Environ. Nanotechnol., 2018, 3(1), 51-57.

[33] Ethiraj A.S., Jayanthi S., Ramalingam C., Banerjee C,. Control of size and antimicrobial activity of green synthesized silver nanoparticles. Mater. Lett., 2016, 185, 526-529.

[34] Jung W.K., Koo H.C., Kim K.W., Shin S., Kim S.H., Park Y.H., Antibacterial activity and mechanism of action of the silver ion in *Staphylococcus aureus* and *Escherichia coli*. Appl. Environ. Microbiol., 2008, 74(7), 2171.

[35] Kędziora A., Speruda M., Krzyżewska E., Rybka J., Łukowiak A., Bugla-Płoskońska G., Similarities and Differences between Silver Ions and Silver in Nanoforms as Antibacterial Agents. Int. J. Mol. Sci., 2018, 19(2), 444.

[36] Ikigai H., Nakae T., Hara Y., Shimamura T., Bactericidal catechins damage the lipid bilayer. BBA-Biomembranes, 1993, 1147(1), 132-136.

[37] Hwang I.S., Hwang J.H., Choi H., Kim K.J., Lee D.G., Synergistic effects between silver nanoparticles and antibiotics and the mechanisms involved. J. Med. Microbiol., 2012, 61(12), 1719-1726.